

Constrained Model-based Relaxation Parameter Mapping using Balanced Steady State Free Precession

Zimu Huo¹, Minghao Zhang², Yiyun Dong³, Joshua Kaggie¹, Pete Lally⁴, Neal Bangerter⁵, Michael Hoff⁶, Martin Graves¹

1. Department of Radiology, University of Cambridge. 2. Wolfson Brain Imaging Centre, University of Cambridge. 3. Department of Physics, University of Washington. 4. Department of Bioengineering, Imperial College London. 5. Department of Electrical and Computer Engineering, Boise State University. 6. Radiology and Biomedical Imaging, University of California, San Francisco.

Introduction: In balanced steady state free precession (bSSFP), the real and imaginary components of the steady-state transverse magnetization form an ellipse across phase cycles on the complex plane. Quantitative parameters may be derived using analytical expressions based on the geometric properties of this ellipse using a method referred to as PLANET¹. However, voxel-wise fitting is sensitive to additive noise, leading to inaccuracies.

We propose estimating relaxation parameters as a constrained nonlinear least square problem subject to data consistency costs in k -space to improve its noise robustness. Unlike traditional methods that extract quantitative relaxation parameters pixel by pixel, our approach leverages global information by jointly estimating T_1 and T_2 across the entire image and assessing reconstruction errors in k -space. Additionally, it supports flexible regularization options, such as total variation, which further mitigates noise sensitivity.

Theory: In this work, we aim to cast the parameter mapping as a constrained nonlinear optimization problem of the standard form:

$$\text{minimize } C(T_1, T_2, M_0, B) = (F \cdot M(T_1, T_2, M_0, B_0) - y)^2 + \lambda R(T_1, T_2, M_0, B_0) \text{ st: } p_i = 0, q_i < 0$$

Here, y signifies the collected data, F denotes the linear Fourier transform operator, and M is a nonlinear operator denoting the bSSFP steady state magnetization at TE. The goal is to jointly estimate the T_1 , T_2 , M_0 , and B_0 maps that best align with the acquired k -space measurement y . p is an equality constraint and q is an inequality constraint on the parameter range. For example, T_1 and T_2 values should be non-negative, and T_1 is always greater than or equal to T_2 in biological tissues. R is an optional regularization function and λ is the regularization parameter. To accelerate the optimization, the analytical gradient and Hessian is provided to the optimization algorithm:

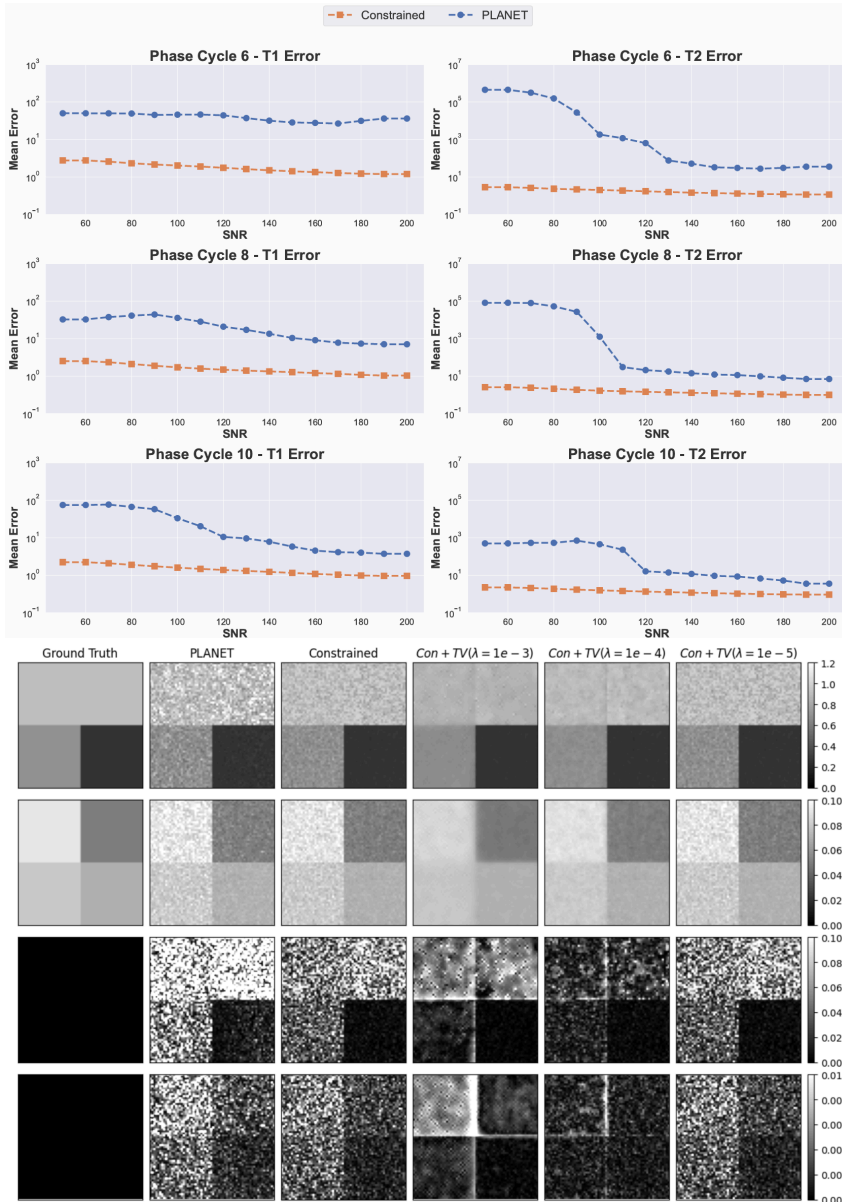
$$\partial C = (\Phi \cdot \partial M)^H \cdot (F \cdot M - y) = (\Phi \cdot J)^H (F \cdot M - y)$$

$$\partial^2 C = (\Phi \cdot J)^H \cdot (\Phi \cdot J) + (\Phi \cdot \nabla J)^H \cdot (F \cdot M - y)$$

J is the Jacobian matrix of the bSSFP steady state equation. $\Phi_{i,j}$ is the Fourier basis function and defined as $\Phi_{i,j} = F\delta_{i,j}$. The δ symbol denotes a 2D Kronecker delta function, resulting in a matrix with a 1 at position (i,j) and 0 elsewhere. Our approach is different by performing the parametric fitting in k -space, where voxel information is correlated through Fourier basis functions. Intuitively, If there exists an overestimated T_1 due to noise for a given voxel, this will propagate to k -space via the Fourier basis function and have a strong penalty in the data consistency cost.

Methods: To evaluate noise sensitivity, we perform a Monte Carlo simulation by randomly generating T_1 , T_2 , and M_0 on a 16 by 16 image patch. T_1 is generated from 100 ms to 3000 ms, T_2 ranges from 1 ms and is upper bounded by the generated T_1 value, and M_0 values range from 0 to 2. B_0 map is generated based on low frequency noise in k -space to create smooth and slowly varying modulations in the image domain. We used a flip angle of 30 degrees, TR of 10 ms, TE of 5 ms. We used conservatively high values of TR to yield a

Figure 1. Noise Sensitivity Analysis. The conventional approach fits each pixel individually across the phase cycle dimension (e.g., fitting through 6 complex data points for 6 phase cycles). In contrast, our method simultaneously fits the entire image by utilizing the entire k-space data across all phase cycles.



worst-case scenario for banding artifacts. We simulated various datasets of 6-10 phase cycles with an increment of 2. The Monte Carlo simulation is repeated 5000 times for each combination of SNR and phase cycles. In the second simulation, we apply total variation as the regularization term on the T_1 and T_2 maps to investigate its effects on a simulated uniform phantom. The optimization is implemented in MATLAB.

Results: In Figure 1, the constrained method consistently shows lower mean errors in T_1 and T_2 estimations across all SNR levels, outperforming the gold standard PLANET method. Figure 2 shows the effect of the total variation. This simulation serves as a proof of concept, illustrating that these regularization techniques can effectively guide the reconstruction process similar to what is observed in image optimization tasks.

Discussion: The proposed method can be extended to multiple coils for parallel imaging. A key advantage is its ability to jointly solve for parameter maps by leveraging information across phase cycles and coils, effectively utilizing data redundancy. One limitation is the assumption of an ideal single-component relaxation model.

Figure 2. Effect of Total Variation. In this simulation, total variation leverages neighboring pixels to better inform the fitting process, further reducing noise sensitivity.

Factors like diffusion, multi-compartment, and magnetization transfer can cause deviation and the steady state equation used in this work cannot fully capture this complexity². It is possible, at least partially, to include these secondary effects into the model. Future work will include phantom and in vivo acquisitions to validate the results.

Conclusions: The proposed constrained model-based fitting approach demonstrates robustness to noise across various phase cycles and SNR levels and outperforms the gold standard PLANET method. This is due to 1) jointly solving parameter maps over an image, 2) constraining the search space, and 3) allowing additional regularizations.

References [1] Y. Shcherbakova. MRM, vol. 81, no. 3, pp. 1534–1552, Oct. 2018 [2] K. Miller. MRM, vol. 63, no. 2, pp. 385–395, Jan. 2010